Original Article

AKT inhibits the phosphorylation level of H2A at Tyr57 via CK2α to promote the progression of gastric cancer

Zhi-Da Chen[1#], Peng-Fei Zhang[2#], Hong-Qing Xi[1], Bo Wei[1], Lin Chen[1]

[1]Department of General Surgery, First Medical Center of Chinese PLA General Hospital, Beijing, China; [2]Department of Oncology, First Medical Center of Chinese PLA General Hospital, Beijing, China

Contributions: (I) Conception and design: ZD Chen, PF Zhang; (II) Administrative support: B Wei, L Chen; (III) Provision of study materials or patients: B Wei, L Chen; (IV) Collection and assembly of data: HQ Xi; (V) Data analysis and interpretation: ZD Chen, PF Zhang; (VI) Manuscript writing: All authors; (VII) Final approval of manuscript: All authors.

[#]These authors contributed equally to this work.

Correspondence to: Lin Chen; Bo Wei. Department of General Surgery, First Medical Center of Chinese PLA General Hospital, 28, Fuxing Road, Haidian District, Beijing 100853, China. Email: chenlinbj@sina.com; weibo@vip.163.com.

Background: Histone H2A and its variants have an important effect on DNA damage repair and cancer development. Protein kinase B (AKT) can regulate various cellular functions and play critical roles in the progression of different cancers. However, the interaction mechanism of H2A with AKT in gastric cancer (GC) has not been reported. A series of experiments were carried out in the present study to investigate this issue.

Methods: Firstly, we used western blot and immunoprecipitation assays to determine the correlation between AKT and H2A, then detected the relationship between AKT and protein kinase CK2α that can phosphorylate H2A at Tyr57 site ($H2A^{Y57}$), and next examined the interaction among AKT, CK2α, and H2A in SNU-16 cells. Subsequently, the effect of these molecules on the cellular proliferation, migration, and invasion was measured by Cell Counting Kit-8 (CCK-8), wound healing, and transwell invasion assays.

Results: Our study preliminarily found that AKT was negatively correlated with H2A phosphorylation at the Tyr 57 site ($H2A^{Y57p}$). It was revealed that AKT mediated the phosphorylation of CK2α at the T13 site, which decreased the affinity of CK2α with its substrate histone H2A and inhibited the level of $H2A^{Y57p}$ in GC cells. Furthermore, AKT-mediated CK2α phosphorylation promoted the proliferation, migration, and invasion of SNU-16 cells possibly through downregulating $H2A^{Y57p}$ level.

Conclusions: These findings contribute to understanding the interactions among AKT, CK2α, and H2A in GC, and provide the potential biomarkers for the diagnosis and treatment of GC.

Keywords: H2A; CK2α; AKT; gastric cancer (GC)

Submitted Apr 22, 2021. Accepted for publication Jul 22, 2021.
doi: 10.21037/jgo-21-260
View this article at: https://dx.doi.org/10.21037/jgo-21-260

Introduction

Gastric cancer (GC) is 1 of the 5 most common cancers in the world and has also been shown to be the second leading cause of death by cancer (1,2). Although the treatment of cancer has improved, the main treatment approach is surgery with chemotherapy, which cannot effectively improve the prognosis and survival rate of patients with GC (3,4). A reason for this is the rapid development of GC and lack of specific clinical symptoms, which makes early diagnosis difficult; another is the high probability of recurrence and metastasis of GC after surgery and due to drug resistance (5,6). Therefore, it is urgent to study the pathogenesis of GC and find new biomarkers for GC treatment.

Epigenetics refers to the study of change in genetic expression that does not alter the DNA sequence but can be inherited (7,8). Post-translational histone modifications are 1 of the most important research directions of epigenetics, which include methylation, ubiquitination, acetylation, and

phosphorylation (9). Histone modifications are implicated in gene expression and play critical roles in regulating cell cycle, DNA replication, and transcription (10). For instance, phosphorylation of histone H2A is associated with many biological processes, including DNA-double-strand-break repair (11,12). Phosphorylation of H2A at Ser121 has been found to prevent chromosome instability (13). The site H2A at Tyr57 ($H2A^{Y57}$) is a new conserved phosphorylation site in H2A, and its phosphorylation ($H2A^{Y57p}$) is mediated by CK2α, which can regulate transcriptional elongation (14). Although histone H2A has been widely reported, a functional understanding of $H2A^{Y57p}$ is still lacking. Many reports have suggested that AKT is closely associated with histone modifications such as acetylation, methylation, and phosphorylation to mediate the progression of cancers (15-17). Park *et al.* indicated that AKT decreases apoptosis by phosphorylation of H2A at threonine-17 under oxidative stress conditions in neurons and PC12 cells (18). However, AKT mediated phosphorylation of H2A at Tyr57 has not been reported, and the relationship between histone H2A phosphorylation at Tyr57 and cancer has rarely been studied. Since AKT and histone H2A are crucial for the development of GC (19-21), we aimed to study the relationship between AKT and the phosphorylation of H2A at Tyr57 to explore the specific molecular mechanism of the AKT/H2A pathway affecting GC, so as to expose new ideas for the prevention and treatment of GC. We present the following article in accordance with the MDAR reporting checklist (available at https://dx.doi.org/10.21037/jgo-21-260).

Methods

Cell culture

Human GC cell lines KATO III, HGC-27, and NCI-N87 were purchased from Nanjing Cobioer Gene Technology Co., Ltd. (Nanjing, China). The SNU-5 and SNU-16 cells were obtained from the American Type Culture Collection (ATCC, Rockville, MD, USA). The MKN-28, MKN-74 cells were purchased from Mingzhou Biotechnology Co., Ltd. (Ningbo, Zhejiang, China). The KATO III and SNU-5 cells were grown in Iscove's Modified Dulbecco's Medium (IMDM) with 10% fetal bovine serum (FBS) (Gibco, Waltham, MA, USA), 1% penicillin-streptomycin (Sangon Biotech, Shanghai, China). Other cell lines were grown in Roswell Park Memorial Institute (RPMI) 1640 medium (Gibco, Waltham, MA, USA) with 10% FBS, 0.1 mg/mL penicillin-streptomycin. All cells were cultured in a humidified incubator at 37 ℃ with 5% CO_2 and 95% humidity.

Western blot

The cells were lysed using lysis buffer (0.5% sodium deoxycholate, 50 mM Tris, pH 7.4, 150 mM NaCl, 1% NP-40) with 20 mg/L DNase on ice for 30 min, and the protein concentration of cell lysates was measured by the bicinchoninic acid (BCA) method. The BCA working solution (A solution: B solution =50:1) was prepared and set for 24 h. A total of 0.5 mg/mL standard protein and the sample protein were diluted and added into a 96-well plate with 20 μL/well, BCA working fluid was added with 200 μL/well, and the absorbance [optical density (OD) =562] was measured after 30 min staining at 37 ℃. Finally, the concentration of sample protein was calculated according to the standard curve. The protein samples were added onto 10% sodium dodecyl sulfate polyacrylamide gel electrophoresis (SDS-PAGE) gel equally for electrophoresis and then transferred onto polyvinylidene fluoride (PVDF) membranes. The membranes were blocked with 5% non-fat milk for 1 h and incubated overnight at 4 ℃ with primary antibodies against: p-CK2α (ab137580, Abcam), H2A (#2578), AKT (#9272), CK2α (#2656), p-AKT (#4058), P-GSK3β (#5558S), T-GSK3β (#5676), HA-tag (#3724), and Myc-tag (#2272, Cell Signaling Technology, Danvers, MA, USA). In addition, the antibody of $H2A^{Y57p}$ was prepared by Biomatik (Kitchener, Ontario, Canada) using the peptide of $H2A^{Y57p}$ (LE (pY) LTAEILELAGNC) as antigen. The membranes were washed with tris buffered saline with Tween 20 (TBST) buffer (to move the unbound proteins), and incubated with the secondary antibodies Goat Anti-Rabbit IgG H&L (HRP) (ab6721) for 1 h at room temperature. The isoform β-actin was used as an internal control. Each experiment was performed in triplicate.

Co-immunoprecipitation (CoIP)

The cells were flushed with phosphate buffered saline (PBS) and lysed in an ice-cold buffer (pH 7.4, 1% Triton X-100, 40 Mm Hepes, 0.1% SDS, 100 mM NaCl, 0.5% Na-deoxycholate, 25 mM β-glycerophosphate, 1 mM ethylenediamine tetraacetic acid (EDTA), 10 μg/mL leupeptin and aprotinin, and 1 mM Na-orthovanadate). The lysates were washed by centrifugation at 25,000 ×g for 20 min, and incubated with antibodies against Myc-CK2α, hemagglutinin (HA)-AKT, CK2α, AKT, and H2A, separately, for 30 min at 4 ℃. Then, the protein A-sepharose bead slurry was added into the lysates and rotation incubated for another 3 h. The immunoprecipitates were rinsed 3 times in ice-cold PBS and added to an SDS-PAGE sample buffer to be boiled for 5 min, followed by

the performance of western blot. The results represented 3 independent experiments.

Cell fractionation experiments

In order to fractionate the cellular proteins into cytoplasmic protein, soluble nucleocytoplasmic proteins and insoluble nucleocytoplasmic proteins (chromatin-binding proteins), SNU-16 cells were resuspended in 400 µL lysis buffer A (Hepes pH 7.9 10 mM, EGTG 0.1 mM, KCl 10 mM, $MgCl_2$ 1.5 mM, EDTA 0.1 mM, and NP-40 0.1 %) and incubated in a shaker incubator for 15 min at 4 ℃. The supernatant (cytoplasm) obtained by centrifugation was discarded, while the sediments were suspended in 125 µL lysis buffer B [Hepes pH 7.9 20 mM, $MgCl_2$ 1.5 mM, NaCl 150 mM, Glyserol 10%, egtazic acid (EGTA) 0.25 mM] and incubated in a shaker incubator for 20 min at 4 ℃. The supernatant was collected as nuclear soluble fraction. Then, the precipitates were resuspended in 250 µL buffer (Tris-HCl pH 7.5 50 mM, NP-40 1%, SDS 0.1%, DOC 0.5%, 150 mM NaCl) and treated with ultrasonication and centrifugation, and the supernatant was insoluble nuclear fraction. The SNU-16 cells in each state were subjected to 3 independent experiments. Finally, the nuclear soluble fraction and the insoluble nuclear fraction (chromatin) were used to implement western blot to explore the affinity between CK2α and H2A.

Cell transfection and treatment

We constructed the plasmids of DN-AKT, constitutively activated-AKT (CA-AKT), $CK2\alpha^{T13A}$, $CK2\alpha^{T13E}$, and siAKT/siCK2α using pEGFP-N1 vector (Sangon Biotech, Shanghai, China). Small interfering RNA (SiRNA) duplexes against AKT, CK2α, and negative control siRNA were purchased from GenePharm Co. Ltd. (Shanghai, China). The cells were cultured overnight in 6-well plates until they were 70–90% confluent, and the cell transfection was implemented according the instructions of Lipofectamine™ LTX Reagent with PLUS™ Reagent (15338030, ThermoFisher, Waltham, MA, USA). The treatment conditions of GC cells when they needed to be treated with hormones were 15 ng/mL of insulin-like growth factor (IGF) for 30 min, or 16 µM of LY294002 for 24 h. The results represented 3 independent experiments.

In vitro kinase activity assay

At a density of 0.2×10^6 cells/mL, SNU-16 cells were transfected with HA-tagged CA-AKT (10 µg). After transfection for 48 h, HA-AKT was immunoprecipitated from the cell lysates, followed by incubation with purified wild-type (WT) or mutant CK2α and kinase reaction mixture with 5 µCi of [γ-^{32}P] ATP and 50 mM cold ATP in kinase buffer at 37 ℃ for 30 min. Reaction was terminated by adding 4× SDS sample loading buffer (10 µL), and the samples were denatured at 95 ℃ for 5 min. The samples were then analyzed by western blot. The image of ^{32}p-labeled proteins was captured by autoradiography. The above same procedures were performed to detect the reaction between WT-, T13A, or T13E-CK2α and H2A. The results represented 3 independent experiments.

Cell proliferation assay

Cell proliferation was measured by Cell Counting Kit-8 (CCK-8) assay. After transfection, SNU-16 cells were collected and inoculated in a 96-well plate (1×10^4 cells per well), followed by incubation in RPMI 1640 medium with 10% FBS at 37 ℃, 5% CO_2 for 24, 48, 72, and 96 h. At the corresponding time point, 10 µL of CCK-8 solution was added to each well of the plate and then incubated for another 4 h in the incubator. The absorbance was measured at 450 nm using a microplate reader. The experiment was repeated 3 times.

Wound healing assay

Cell migration was measured using a wound healing assay. After transfection, SNU-16 cells were cultured in 6-well plates to 100% confluence, and then the cell monolayer was scratched using a sterile 100 µL pipette tip in a straight line. Next, the cells were washed with PBS and incubated in RPMI 1640 medium without serum for 24 h at 37 ℃, 5% CO_2. The images of the cells were visualized using a light microscope (Olympus BX51, Olympus Corporation, Tokyo, Japan; magnification, ×100). The results represented 3 independent experiments.

Transwell invasion assay

Cell invasion was analyzed by transwell chamber. The cells were digested by pancreatin and resuspended in serum-free RPMI 1640 medium. After the lower compartment was filled with complete medium, the 4×10^4 cells were added into the upper compartment of a transwell chamber (8 µm pore; BD Biosciences, Becton, Dickinson and Company, San Jose, CA, USA) pre-coated with Matrigel and cultured for 24 h at 37 ℃. Then, the cells on the top surface of the chamber were wiped off with a cotton swab, the cells that invaded the lower side of the chamber were fixed with 5% glutaraldehyde for 15 min and stained with crystal violet for 10 min. Finally, the cells were

counted under light microscope (Olympus BX51, Olympus Corporation, magnification, ×200). The results represented 3 independent experiments.

Analysis of apoptosis

SUN-16 cells that cultured in the 6-well plates were washed with PBS and digested by trypsin. After the digestion was stopped, the cells were washed with PBS, and the cells were collected by centrifuging at 200 ×g for 5 min. Next, Annexin V-FITC binding solution was used to resuspend the cells, and the cells were incubated at room temperature and dark for 10 min, and then the cells were collected by centrifuging at 200 ×g for 5 min. The cells were then resuspend with Annexin V-FITC binding solution and co-cultured with the propidium iodide (PI) on ice and dark for 10 min. Finally, cells were determined for early and late apoptosis by using a BD FACSCalibur flow cytometer (Bedford, MA) and the data were analyzed by GraphPad Prism 7.0.

Statistical analysis

Data were presented as the mean ± standard error of the mean (SEM), and each experiment was repeated in triplicate. The software GraphPad Prism 7.0 (San Diego, CA, USA) was used to analyze the data. We performed statistical analysis according to analysis of variance (ANOVA) followed by Sidak's multiple comparisons test when datasets contained multiple groups, and the comparison between the 2 groups was statistically analyzed according to *t*-test. A P value <0.05 was considered statistically significant.

Results

AKT inversely regulates H2A^{Y57p}

Western blot assay was performed to verify the relationship between p-AKT and H2A^{Y57p}. We discovered that GC cells with lower levels of H2A^{Y57p} usually had high levels of p-AKT (*Figure 1A*). Thus, the expression levels of H2A^{Y57p} were negatively correlated with p-AKT levels. This negative correlation prompted us to detect whether alteration of AKT activity can change the expression of H2A^{Y57p}. It was shown that IGF as an activator of AKT could increase the level of p-AKT but inhibit the level of H2A^{Y57p}, while the addition of the PI3K-AKT inhibitor, LY294002, could reverse this effect (*Figure 1B*). Similarly, the level of H2A^{Y57p} was increased in cells transfected by dominant negative AKT (DN-AKT) or AKT siRNA (*Figure 1C,1D*). Additionally, the correlation between AKT activity and the level of H2A^{Y57p} was further verified by changing the treatment duration of LY294002. The results showed that the level of H2A^{Y57p} displayed an increasing trend over time, while the level of p-AKT had the opposite trend (*Figure 1E*). In conclusion, AKT could negatively regulate the phosphorylation level of H2A^{Y57}.

AKT phosphorylates CK2α on T13 site

To further explore the molecular mechanism, we attempted to study the relationship between AKT and CK2α on account CK2α having been shown to phosphorylate Tyr 57 in H2A (H2A^{Y57}) (14). Firstly, CoIP experiments were performed to detect whether CK2α is the target of AKT. The results showed that CK2α is associated with CA-AKT but not DN-AKT (*Figure 2A*). Furthermore, the association between endogenous AKT and CK2α was also found, and this association was decreased in the cells treated with LY294002 (*Figure 2B*). Thus, these results suggested that CK2α was the target of AKT and they could interact in GC cells.

Secondly, to determine whether AKT can phosphorylate CK2α, we applied the PhosphoSitePlus (https://www.phosphosite.org/homeAction.action) and Scansite (https://scansite4.mit.edu/4.0/#home) websites to find the AKT phosphorylation sites in CK2α, and obtained 1 potential site, T13. An *in vitro* kinase assay was performed to detect the interaction of HA-tagged AKT with WT CK2α and mutants of CK2α in which the phosphorylation site T13 was replaced by Ala or Glu (T13A and T13E) and glutathione S-transferase (GST). The results indicated that AKT could phosphorylate WT CK2α but not CK2α mutants (*Figure 2C*). To verify that AKT can indeed phosphorylate CK2α at T13 site *in vivo*, we synthesized an antibody, which specifically recognized p-CK2α at the T13 site but failed to detect an unphosphorylated CK2α or an unrelated peptide (Figure S1). Thus, we speculated that AKT could phosphorylate CK2α at T13 site.

Thirdly, to further verify the relationship between AKT and p-CK2α, the endogenous and exogenous CK2α levels were determined by immunoprecipitation and western blot after SNU-16 cells had been treated with an AKT inhibitor (LY294002 or DN-AKT) or transfected with CK2α plasmid. After SNU-16 cells were treated with LY294002 or DN-AKT, endogenous CK2α was immunoprecipitated using a CK2α antibody and subjected to western blot using a p-CK2α antibody (*Figure 2D*). The p-CK2α was observed in SNU-16 cells without LY294002 treatment, and it was not found in cells treated with LY294002 or transfected with DN-AKT (*Figure 2D*). When SNU-16 cells were immunoprecipitated with a p-CK2α antibody,

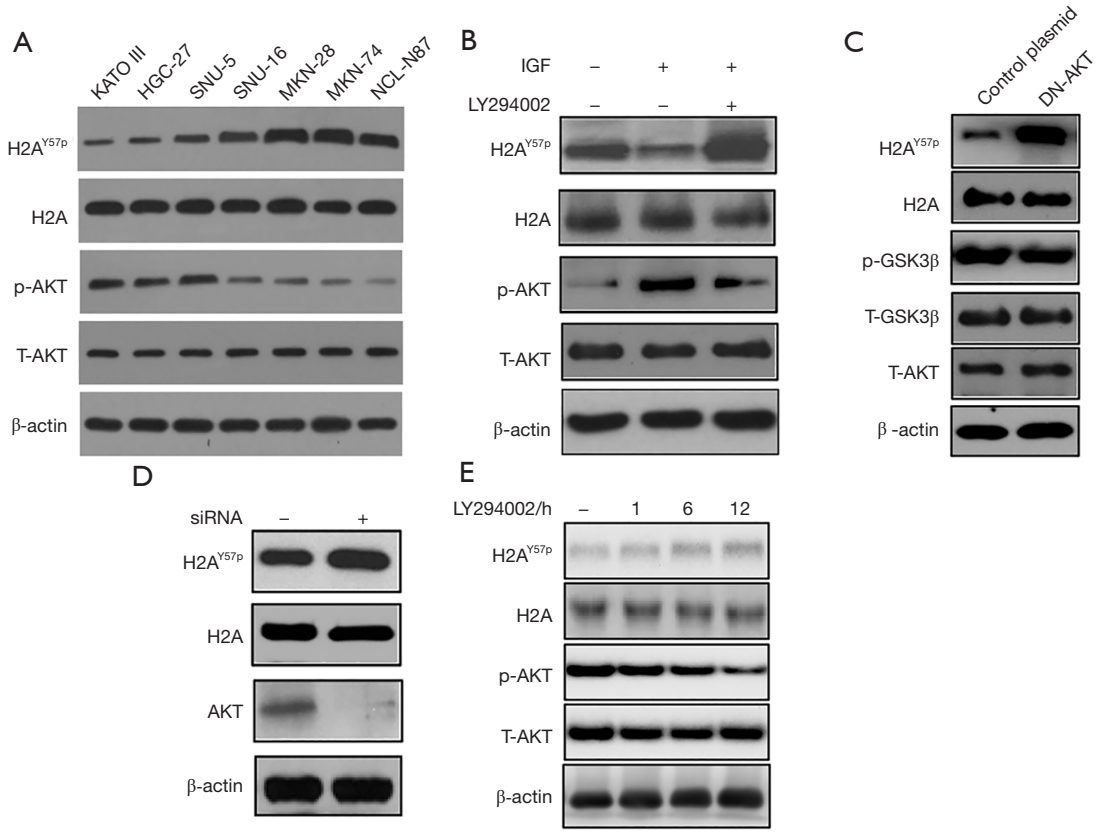

Figure 1 AKT inversely regulates $H2A^{Y57p}$. (A) $H2A^{Y57p}$ and p-AKT in different cell lines were assessed by western blot. (B) SNU-16 cells were treated with IGF and LY294002, and western blot was used to test the levels of $H2A^{Y57p}$ and p-AKT in the SNU-16 cell lines treated with the AKT inhibitor (LY294002) or an activator of AKT (IGF). (C) The level of $H2A^{Y57p}$ was determined using western blot in SNU-16 cells transfected by DN-AKT plasmid or control plasmid. The p-GSKβ was used as a control for AKT activity. (D) A western blot analysis of $H2A^{Y57p}$ in SNU-16 cells transfected with siRNA of AKT or siRNA control for 48 h. (E) The level of $H2A^{Y57p}$ were measured by western blot assay in SNU-5 cells that were treated with LY294002 for 1 h, 6 h, and 12 h. AKT, protein kinase B; IGF, insulin-like growth factor; DN-AKT, dominant negative AKT; siRNA, small interfering RNA.

the same lysates were measured using western blot with a CK2α antibody (*Figure 2E*). The results displayed in *Figure 2E* also indicated that p-CK2α expression was blocked when AKT activity was inhibited by LY294002 or DN-AKT. Additionally, after SNU-16 cells were transfected with mutant (MUT-) CK2α plasmid (T13A-CK2α plasmid, mimicking the unphosphorylated state) or treated with WT-CK2α plasmid and LY294002, exogenous CK2α levels were detected by immunoprecipitation and western blot assays. The results revealed that the expression of p-CK2α could be blocked by LY294002 in SNU-16 cells transfected with $CK2α^{WT}$, and its expression was also suppressed by $CK2α^{T13A}$ plasmid (*Figure 2F*). Collectively, these findings supported that AKT interacts with CK2α in cells, and AKT phosphorylated CK2α at the T13 site.

The AKT-mediated phosphorylation of CK2α inhibits the phosphorylation of $H2A^{Y57}$

We studied whether AKT-mediated phosphorylation of CK2α could affect the phosphorylation of $H2A^{Y57}$. Firstly, CA-AKT decreased the level of $H2A^{Y57p}$, whereas DN-AKT increased the level of $H2A^{Y57p}$ (*Figure 3A*). Thus, the activity of AKT was negatively correlated with the level of $H2A^{Y57}$ phosphorylation ($H2A^{Y57p}$). Secondly, the level of $H2A^{Y57p}$ in cells transfected with T13A-CK2α was significantly higher than that in cells transfected with WT-CK2α or T13E-CK2α (mimicking the phosphorylated state) (*Figure 3B*). Hence, the level of p-CK2α was negatively correlated with the level of $H2A^{Y57p}$. Thirdly, the increase of $H2A^{Y57p}$ expression caused by DN-AKT was reversed by knockdown of CK2α (siRNA

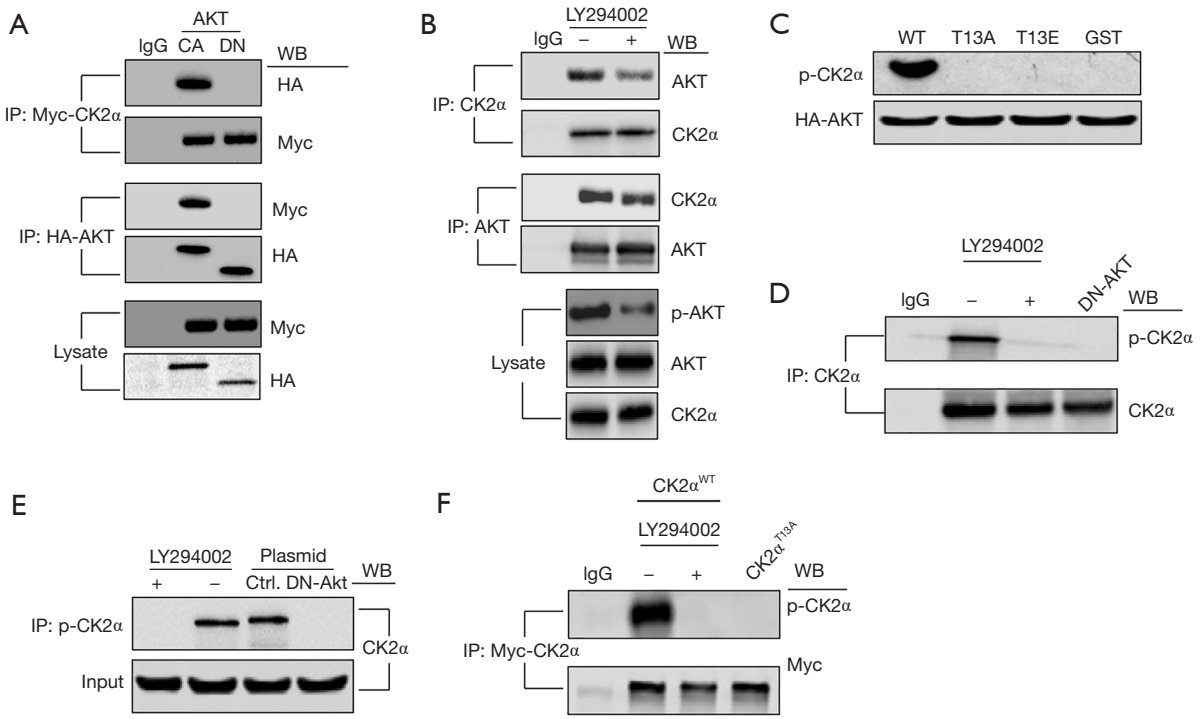

Figure 2 AKT phosphorylates CK2α on T13 site. (A) Co-immunoprecipitation analysis of CK2α and AKT. The lysates of SNU-16 cells transfected with the plasmids (CA-AKT or DN-AKT) were analyzed by immunoprecipitation with antibodies against HA or Myc. Meanwhile, western blot analysis was performed to detect the expression of CK2α and AKT in whole cell lysates. The DN-AKT is a mutant that cannot be activated and can inhibit the activation of wild-type AKT in cells. The CA-AKT is a mutant with spontaneous and persistent activation. (B) The interaction between endogenous CK2α and AKT in SNU-16 cells was detected by immunoprecipitation and western blot assays (± LY294002). (C) HA-tagged AKT was expressed in SNU-16 cells and collected by immunoprecipitation. The interaction of HA-tagged AKT with WT-CK2α and mutants of CK2α (T13A, T13E, and GST) was measured by an *in vitro* kinase assay. (D) Endogenous CK2αfrom SNU-16 (± LY294002) or DN-AKT/SNU-16 cells was analyzed by immunoprecipitation with an anti-CK2α antibody, and then analyzed with western blot using an antibody against p-CK2α. (E) After SNU-16 cells were treated with LY294002 or DN-AKT, they were immunoprecipitated with a p-CK2α antibody, and the same cell lysates were measured using western blot with a CK2α antibody. (F) SNU-16 cells were transfected with WT-CK2α (± LY294002) or T13A-CK2α, the exogenous CK2α was determined by immunoprecipitation, and was subjected to western blot with an antibody against p-CK2α. AKT, protein kinase B; CA-AKT, constitutively activated-AKT; DN-AKT, dominant negative AKT; WT, wild-type.

CK2α, si-CK2α) (*Figure 3C*). Therefore, AKT-mediated phosphorylation of CK2αinhibited the level of $H2A^{Y57p}$.

This result was further verified by *in vitro* the kinase activity assays. As shown in *Figure 3D*, AKT could not phosphorylate mutant CK2α at the T13 site (CK2α-T13A) and only phosphorylated WT-CK2α. In addition, the phosphorylation of CK2α (p-CK2α) decreased the level of $H2A^{Y57p}$. To further confirm this finding, a kinase activity assay was performed on WT-, T13A, or T13E-CK2α, and H2A expressed *in vitro*. The unphosphorylated state of CK2α (T13A-CK2α) and its normal state (WT-CK2α) could enhance the level of $H2A^{Y57p}$ as compared to the control group, but the phosphorylated state of CK2α (T13E-CK2α) decreased the level of $H2A^{Y57p}$ compared with the WT-CK2α and T13A-CK2α groups (*Figure 3E*). Therefore, the above experimental data indicated that AKT-mediated phosphorylation of CK2α can inhibit the level of $H2A^{Y57p}$.

AKT-mediated phosphorylation of CK2α changes substrate affinity

To test whether AKT-mediated phosphorylation changed the affinity of CK2α with its substrate histone H2A, a CoIP assay was performed to determine the combination

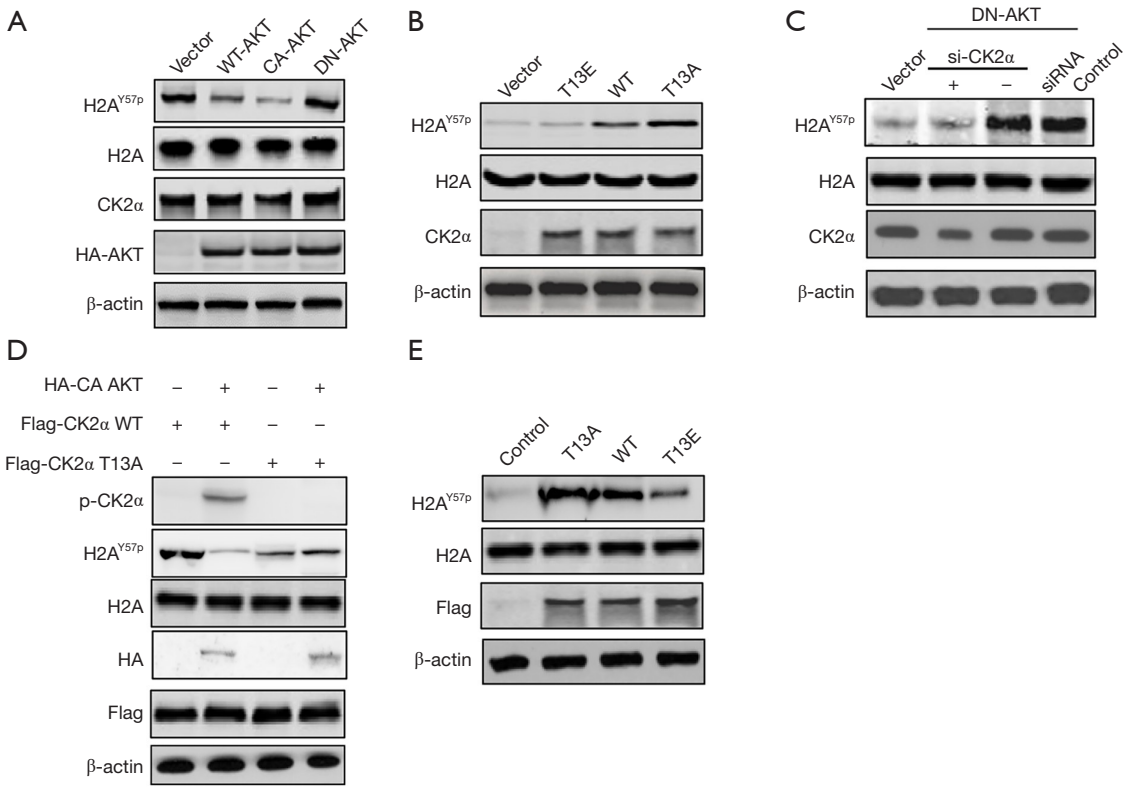

Figure 3 The AKT-mediated phosphorylation of CK2α inhibits the phosphorylation of $H2A^{Y57}$. (A) SNU-16 cells were co-transfected with CK2α and WT-AKT, CA-AKT or DN-AKT plasmids. Samples were collected after 48 h of transfection and analyzed by western blot. (B) SNU-16 cells were transfected with WT- or MUT-CK2α (T13A, T13E). Samples were collected after 48 h of transfection and analyzed by western blot. (C) DN-AKT/SNU-16 cells were transfected by control (ctrl) or siRNA CK2α. Samples were collected after 48 h of transfection and analyzed by western blot. (D) HA-CA-AKT immunoprecipitated from unstimulated cell lysates was mixed with FLAG-tagged WT-CK2α or the T13A mutant and then analyzed by performing a kinase activity assay. (E) FLAG-tagged WT-CK2α, T13E, or T13A mutant were expressed *in vitro* and immunopurified with an anti-FLAG antibody. Kinase activity was then assayed. AKT, protein kinase B; CA-AKT, constitutively activated-AKT; DN-AKT, dominant negative AKT; WT, wild-type; siRNA, small interfering RNA.

of histone H2A with CK2α. The experimental results suggested that T13A-CK2α showed a greater correlation with H2A as compared to WT- or T13E-CK2α, but the correlation between WT-CK2α with H2A was enhanced after LY294002 treatment (*Figure 4A*). Additionally, insoluble (chromatin-bound, c) and soluble (s) nuclear fractions were isolated from SNU-16 cells treated with LY294002, DN-AKT, or IGF. Reduced AKT activity caused by LY294002 or DN-AKT increased the amount of chromatin-bound CK2α but decreased the level of soluble CK2α (*Figure 4B*). Furthermore, activation of AKT induced by IGF decreased chromatin-bound CK2α but increased soluble CK2α, whereas this situation was reversed by the introduction of LY294002 (*Figure 4C*). Therefore, AKT-mediated CK2α phosphorylation reduced the affinity of CK2α with its substrate histone H2A, which resulted in a decrease of $H2A^{Y57p}$ level.

Downregulated of $H2A^{Y57p}$ induced by AKT-mediated CK2α phosphorylation promotes cell proliferation, migration, and invasion

To validate whether downregulation of $H2A^{Y57p}$ induced by AKT-mediated p-CK2α can affect the growth of GC cells, we performed CCK-8, wound healing, transwell invasion assays and apoptosis assays on the transfected SNU-16 cells. Firstly, after SNU-16 cells were transfected with control vectors, CA-AKT, CA-AKT+T13A-CK2α, DN-AKT, and DN-AKT+T13E-CK2α, the protein expression of $H2A^{Y57p}$ was determined by western blot (*Figure 5A*). The level of

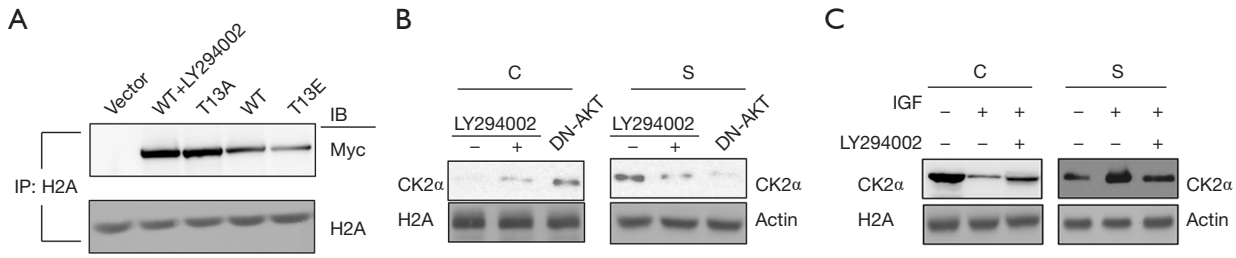

Figure 4 AKT-mediated phosphorylation of CK2α changes substrate affinity. (A) Co-immunoprecipitation of endogenous histone H2A and WT- or MUT-CK2α (T13A, T13E) from SNU-16 cells. (B,C) The endogenous CK2α in soluble (s) and chromatin-bound (c) was analyzed by western blotting, with constituents fractions used in western blot from SNU-16 (± LY294002) and DN-AKT/SNU-16 cells (B) or from SNU-16 cells (C) treated with IGF or processed successively by IGF and LY294002. AKT, protein kinase B; DN-AKT, dominant negative AKT; WT, wild-type; IGF, insulin-like growth factor.

$H2A^{Y57p}$ was decreased by the activation of AKT (CA-AKT transfection) compared with the control group and yet this situation was changed by the co-transfection of CA-AKT with T13A-CK2α (*Figure 5A*). Besides, the increase of $H2A^{Y57p}$ level caused by the inhibition of AKT activity (DN-AKT transfection) was reversed by the introduction of T13E-CK2α (*Figure 5A*). Secondly, the CCK-8 assay indicated that the promotion of SNU-16 cell proliferation induced by CA-AKT was suppressed by the introduction of T13A-CK2α, and the inhibition of the cell proliferation caused by DN-AKT was improved after SNU-16 cells were co-transfected with DN-AKT and T13E-CK2α (*Figure 5B*). Thirdly, wound healing and transwell invasion assays showed that CA-AKT obviously promoted the migration and invasion of SNU-16 cells in comparison to the control group but the introduction of T13A-CK2α suppressed the increase tendency (*Figure 5C,5D*). In addition, the inhibition of the cell migration and invasion caused by DN-AKT was improved by T13E-CK2α co-transfected with DN-AKT into SNU-16 cells (*Figure 5C,5D*). Finally, the results of apoptosis assay indicated that CA-AKT and T13E-CK2α decreased the apoptosis rate, while DN-AKT and T13A-CK2α increased it (*Figure 5E*). Therefore, the change of $H2A^{Y57p}$ level was associated with the growth and metastasis of SNU-16 cells, and consequently we speculated that AKT-mediated CK2α phosphorylation promoted the proliferation, migration, invasion and inhibited the apoptosis of SNU-16 cells possibly through downregulating $H2A^{Y57p}$ level.

Discussion

Our study indicated that AKT-mediated phosphorylation of CK2α at the T13 site inhibited the phosphorylation level of histone H2A at the Y57 site in GC cells. Besides, the enhanced phosphorylation of CK2α decreased the affinity of CK2α with its substrate histone H2A, resulting in a decreased $H2A^{Y57p}$ level. Furthermore, AKT-mediated CK2α phosphorylation promoted the proliferation, migration, and invasion of SNU-16 cells possibly through downregulating the $H2A^{Y57p}$ level.

Serine/threonine kinase AKT is one of the main downstream targets of the phosphatidylinositol 3 kinase (PI3K) pathway (22), which mediates a series of survival promoting signals, such as proliferation, anti-apoptosis, angiogenesis, and cell growth (23). The abnormal activation of AKT is related to the occurrence of a variety of diseases and the chemoresistance of tumors (22,24). Furthermore, AKT also participates in histone modifications to mediate the progression and development of cancers (15,16). The Ras-AKT signaling pathway promotes the progression of glioma through inhibiting the phosphorylation of histone H1.5 (17). It has been shown that AKT can control H3K4 methylation to modulate the breast cancer epigenome (25). Thus, the interaction between AKT and histone modifications in cancers has attracted increasing attention.

Histones are mainly composed of 4 kinds of core histone including H2A, H2B, H3, and H4, which play an important regulatory role in the genome (26). It has been reported that the post-translational modification mechanism of histone H2A and its variants has a certain impact on DNA damage repair and the occurrence and development of cancer. For instance, the ubiquitination mechanism of H2A inhibits transcription activity and DNA damage repair activity, thus increasing the incidence of breast and ovarian cancers (27). The high expression of histone variant H2A.

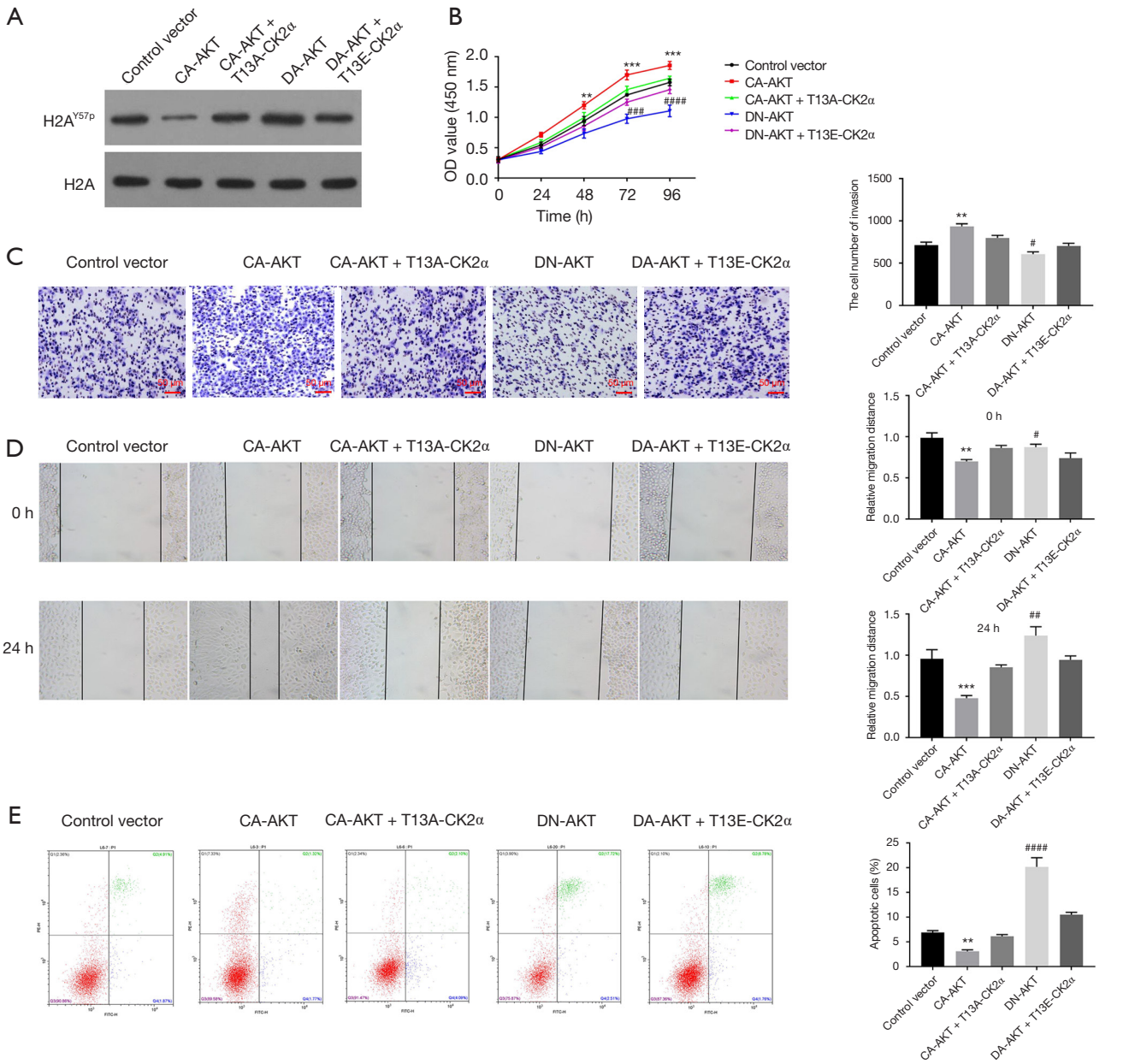

Figure 5 Downregulated of $H2A^{Y57p}$ induced by AKT-mediated CK2α phosphorylation promotes cell proliferation, migration and invasion. After SNU-16 cells were transfected with a control vector, CA-AKT, CA-AKT+T13A-CK2α, DN-AKT, DN-AKT+T13E-CK2α, (A) the protein expression of $H2A^{Y57p}$ was determined by western blot; (B) the proliferation of SNU-16 cells was detected using CCK-8 assay; (C) the cellular invasion was measured with transwell invasion assay (Crystal Violet Staining, scale 50 μm); (D) the cellular migration was assessed using wound healing assay. (E) the apoptotic rate was detected by flow cytometry. **, P<0.01, ***, P<0.001 *vs.* CA-AKT+T13A-CK2α group; #, P<0.05, ##, P<0.01, ###, P<0.001, ####, P<0.0001 *vs.* DN-AKT+T13E-CK2α. AKT, protein kinase B; CA-AKT, constitutively activated-AKT; DN-AKT, dominant negative AKT; CCK-8, Cell Counting Kit-8.

Z in breast cancer and its antagonism to DNA methylation may lead to gene silencing, including the silence of tumor suppressor genes (28). The phosphorylation level of histone variant H2A.X can regulate the progress of cancer, and can also serve as a biomarker of cancer prognosis and treatment evaluation (29). The site H2A at Tyr57 ($H2A^{Y57}$), a new

conserved phosphorylation site in H2A, is able to mediate transcriptional elongation via CK2α regulation (14). To date, there are few reports regarding the interaction of H2A with AKT. To explore this issue, our study first found that AKT was negatively correlated with the phosphorylation level of H2A at Tyr57 site ($H2A^{Y57}$) in GC cells.

We further explored the detailed mechanism between $H2A^{Y57}$ and AKT. On one hand, the phosphorylation of the H2A at Y57 site is mediated by CK2α (14,30). On the other hand, the aberrant expression of CK2α is also correlated to tumor; for instance, Wu *et al*. found that CK2α knockout can inhibit the migration and invasion of liver cancer cells (31); Liu *et al*. found that CK2α levels in non-small cell lung cancer cells increased abnormally (32), and Zhang *et al*. showed that over expression of CK2α promotes the development of human malignant pleural mesothelioma (33). Hence, we speculated that AKT might interact with CK2α to regulate $H2A^{Y57}$ phosphorylation, and their interaction could be involved in the progression of GC. In order to confirm this hypothesis, we carried out CoIP and western blotting experiments, and the results showed that AKT inhibited the phosphorylation of $H2A^{Y57}$ by phosphorylating CK2α. In addition, enhanced phosphorylation of CK2α decreased the affinity of CK2α with its substrate histone H2A, leading to a decrease of $H2A^{Y57p}$ level. Moreover, AKT-mediated CK2α phosphorylation promoted the proliferation, migration, and invasion of GC cells possibly through downregulating $H2A^{Y57p}$ level.

Conclusions

In conclusion, AKT can phosphorylate CK2α at the T13 site, which decreases the affinity of CK2α with its substrate histone H2A and inhibits the phosphorylation of $H2A^{Y57}$. Moreover, the interaction among AKT, CK2α, and H2A affected the proliferation, migration, and invasion of GC cells. Therefore, these molecules are effective biological targets for the treatment of GC, and provide new ideas for understanding the pathogenesis of GC.

Acknowledgments

Funding: This work was supported by grants from the National Nature Science Foundation of China (81972790, 81672319, 81602507, 81773135, and 81572465).

Footnote

Reporting Checklist: The authors have completed the MDAR reporting checklist. Available at https://dx.doi.org/10.21037/jgo-21-260

Data Sharing Statement: Available at https://dx.doi.org/10.21037/jgo-21-260

Conflicts of Interest: All authors have completed the ICMJE uniform disclosure form (available at https://dx.doi.org/10.21037/jgo-21-260). Dr. LC reported that this work was supported by grants from the National Nature Science Foundation of China (81972790, 81672319, 81602507, 81773135, and 81572465). The other authors have no conflicts of interest to declare.

Ethical Statement: The authors are accountable for all aspects of the work in ensuring that questions related to the accuracy or integrity of any part of the work are appropriately investigated and resolved. The study was conducted in accordance with the Declaration of Helsinki (as revised in 2013). Institutional ethical approval and informed consent were waived.

References

1. Kamangar F, Dores GM, Anderson WF. Patterns of cancer incidence, mortality, and prevalence across five continents: defining priorities to reduce cancer disparities in different geographic regions of the world. J Clin Oncol 2006;24:2137-50.
2. Zhou Q, Wu X, Wang X, et al. The reciprocal interaction between tumor cells and activated fibroblasts mediated by TNF-alpha/IL-33/ST2L signaling promotes gastric cancer metastasis. The reciprocal interaction between tumor cells and activated fibroblasts mediated by TNF-α/IL-33/ST2L signaling promotes gastric cancer metastasis. Oncogene 2020;39:1414-28.
3. Sakuramoto S, Sasako M, Yamaguchi T, et al. Adjuvant chemotherapy for gastric cancer with S-1, an oral fluoropyrimidine. N Engl J Med 2007;357:1810-20.
4. Bang YJ, Kim YW, Yang HK, et al. Adjuvant capecitabine and oxaliplatin for gastric cancer after D2 gastrectomy (CLASSIC): a phase 3 open-label, randomised controlled trial. Lancet

2012;379:315-21.
5. Tsujimoto H, Ono S, Ichikura T, et al. Roles of inflammatory cytokines in the progression of gastric cancer: friends or foes? Gastric Cancer 2010;13:212-21.
6. Chia NY, Tan P. Molecular classification of gastric cancer. Ann Oncol 2016;27:763-9.
7. Waddington CH. The epigenotype. 1942. Int J Epidemiol 2012;41:10-3.
8. Tsou PS, Sawalha AH. Unfolding the pathogenesis of scleroderma through genomics and epigenomics. J Autoimmun 2017;83:73-94.
9. Handy DE, Castro R, Loscalzo J. Epigenetic modifications: basic mechanisms and role in cardiovascular disease. Circulation 2011;123:2145-56.
10. Stillman B. Histone Modifications: Insights into Their Influence on Gene Expression. Cell 2018;175:6-9.
11. Jbara M, Maity SK, Morgan M, et al. Chemical Synthesis of Phosphorylated Histone H2A at Tyr57 Reveals Insight into the Inhibition Mode of the SAGA Deubiquitinating Module. Angew Chem Int Ed Engl 2016;55:4972-6.
12. Sharma A, Singh K, Almasan A. Histone H2AX phosphorylation: a marker for DNA damage. Methods Mol Biol 2012;920:613-26.
13. Kawashima SA, Yamagishi Y, Honda T, et al. Phosphorylation of H2A by Bub1 prevents chromosomal instability through localizing shugoshin. Science 2010;327:172-7.
14. Basnet H, Su XB, Tan Y, et al. Tyrosine phosphorylation of histone H2A by CK2 regulates transcriptional elongation. Nature 2014;516:267-71.
15. Lee JV, Carrer A, Shah S, et al. Akt-dependent metabolic reprogramming regulates tumor cell histone acetylation. Cell Metab 2014;20:306-19.
16. Cha TL, Zhou BP, Xia W, et al. Akt-mediated phosphorylation of EZH2 suppresses methylation of lysine 27 in histone H3. Science 2005;310:306-10.
17. Sang B, Sun J, Yang D, et al. Ras-AKT signaling represses the phosphorylation of histone H1.5 at threonine 10 via GSK3 to promote the progression of glioma. Artif Cells Nanomed Biotechnol 2019;47:2882-90.
18. Park JH, Kim CK, Lee SB, et al. Akt attenuates apoptotic death through phosphorylation of H2A under hydrogen peroxide-induced oxidative stress in PC12 cells and hippocampal neurons. Sci Rep 2016;6:21857.
19. Dong C, Sun J, Ma S, et al. K-ras-ERK1/2 down-regulates H2A.X(Y142ph) through WSTF to promote the progress of gastric cancer. BMC Cancer 2019;19:530.
20. Yang WY, Gu JL, Zhen TM. Recent advances of histone modification in gastric cancer. J Cancer Res Ther 2014;10 Suppl:240-5.
21. Singh SS, Yap WN, Arfuso F, et al. Targeting the PI3K/Akt signaling pathway in gastric carcinoma: A reality for personalized medicine? World J Gastroenterol 2015;21:12261-73.
22. Manning BD, Toker A. AKT/PKB Signaling: Navigating the Network. Cell 2017;169:381-405.
23. Hasselblom S, Hansson U, Olsson M, et al. High immunohistochemical expression of p-AKT predicts inferior survival in patients with diffuse large B-cell lymphoma treated with immunochemotherapy. Br J Haematol 2010;149:560-8.
24. Manning BD, Cantley LC. AKT/PKB signaling: navigating downstream. Cell 2007;129:1261-74.
25. Spangle JM, Dreijerink KM, Groner AC, et al. PI3K/AKT Signaling Regulates H3K4 Methylation in Breast Cancer. Cell Rep 2016;15:2692-704.
26. Conerly ML, Teves SS, Diolaiti D, et al. Changes in H2A.Z occupancy and DNA methylation during B-cell lymphomagenesis. Genome Res 2010;20:1383-90.
27. Stewart MD, Zelin E, Dhall A, et al. BARD1 is necessary for ubiquitylation of nucleosomal histone H2A and for transcriptional regulation of estrogen metabolism genes. Proc Natl Acad Sci U S A 2018;115:1316-21.
28. Hua S, Kallen CB, Dhar R, et al. Genomic analysis of estrogen cascade reveals histone variant H2A.Z associated with breast cancer progression. Mol Syst Biol 2008;4:188.
29. Corujo D, Buschbeck M. Post-Translational Modifications of H2A Histone Variants and Their Role in Cancer. Cancers (Basel) 2018;10:59.
30. Sueoka T, Hayashi G, Okamoto A. Regulation of the Stability of the Histone H2A-H2B Dimer by H2A Tyr57 Phosphorylation. Biochemistry 2017;56:4767-72.
31. Wu D, Sui C, Meng F, et al. Stable knockdown of protein kinase CK2-alpha (CK2alpha) inhibits migration and invasion and induces inactivation of hedgehog signaling pathway in hepatocellular carcinoma Hep G2 cells. Acta Histochem 2014;116:1501-8.
32. Liu Y, Amin EB, Mayo MW, et al. CK2alpha' Drives Lung Cancer Metastasis by Targeting BRMS1 Nuclear Export and Degradation. Cancer Res 2016;76:2675-86.
33. Zhang S, Yang YL, Wang Y, et al. CK2alpha, over-expressed in human malignant pleural mesothelioma, regulates the Hedgehog signaling pathway in mesothelioma cells. J Exp Clin Cancer Res 2014;33:93.

(English Language Editor: J. Jones)

Cite this article as: Chen ZD, Zhang PF, Xi HQ, Wei B, Chen L. AKT inhibits the phosphorylation level of H2A at Tyr57 via CK2α to promote the progression of gastric cancer. J Gastrointest Oncol 2021;12(4):1363-1373. doi: 10.21037/jgo-21-260

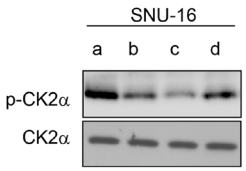

Figure S1 Specificity of the anti-p-CK2α antibody. (a, b) The levels of phospho-CK2α from SNU-16 cells transfected with DN-AKT plasmid or scramble plasmid (control) were determined using western blot. (c, d) The levels of phospho-CK2α from SNU-16 cells were detected by western blot. The antibody was introduced using peptide competition processes, among which the antibody against p-CK2α was pre-incubated with phospho-CK2α or non-phospho-CK2α peptides. a: control, b: DN-AKT transfection; c: the p-CK2α antibody was pre-incubated with phospho-CK2α; d: the p-CK2α antibody was pre-incubated with non-phospho-CK2α peptides. AKT, protein kinase B; CA-AKT, constitutively activated-AKT; DN-AKT, dominant negative AKT.

https://dx.doi.org/10.21037/jgo-21-260